Article

Proton-Coupled Electron Transfer in a Model for Tyrosine Oxidation in Photosystem II

Claudio Carra, Nedialka Iordanova, and Sharon Hammes-Schiffer

J. Am. Chem. Soc., **2003**, 125 (34), 10429-10436• DOI: 10.1021/ja035588z • Publication Date (Web): 01 August 2003

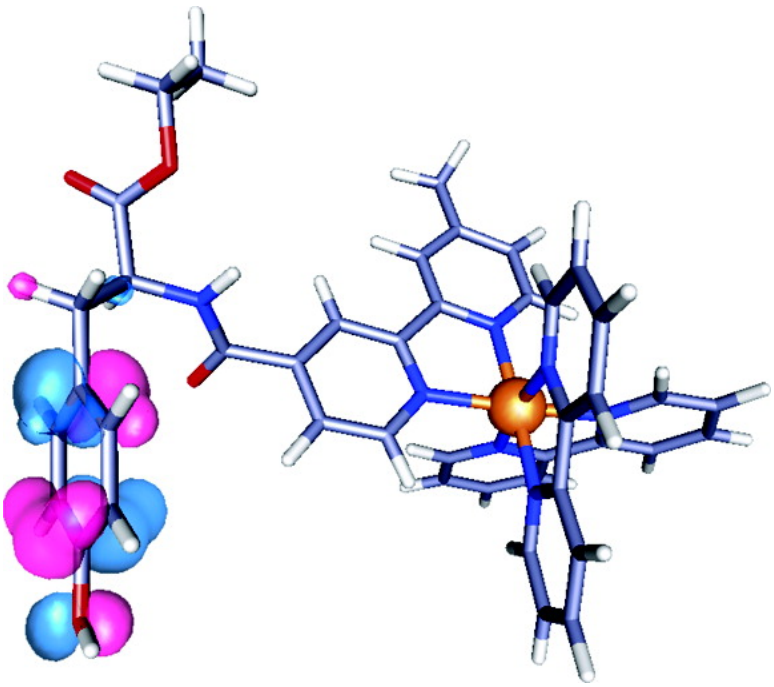

J|A|C|S
ARTICLES
Published on Web 08/01/2003

Proton-Coupled Electron Transfer in a Model for Tyrosine Oxidation in Photosystem II

Claudio Carra, Nedialka Iordanova, and Sharon Hammes-Schiffer*

Contribution from the Department of Chemistry, 152 Davey Laboratory, Pennsylvania State University, University Park, Pennsylvania, 16802

Received April 11, 2003; E-mail: shs@chem.psu.edu

Abstract: Theoretical calculations of a model for tyrosine oxidation in photosystem II are presented. In this model system, an electron is transferred to ruthenium from tyrosine, which is concurrently deprotonated. This investigation is motivated by experimental measurements of the dependence of the rates on pH and temperature (Sjödin et al. *J. Am. Chem. Soc.* **2000**, *122*, 3932). The mechanism is proton-coupled electron transfer (PCET) at pH < 10 when the tyrosine is initially protonated and is single electron transfer (ET) for pH > 10 when the tyrosine is initially deprotonated. The PCET rate increases monotonically with pH, whereas the single ET rate is independent of pH and is 2 orders of magnitude faster than the PCET rate. The calculations reproduce these experimentally observed trends. The pH dependence for the PCET reaction arises from the decrease in the reaction free energies with pH. The calculations indicate that the larger rate for single ET arises from a combination of factors, including the smaller solvent reorganization energy for ET and the averaging of the coupling for PCET over the reactant and product hydrogen vibrational wave functions (i.e., a vibrational overlap factor in the PCET rate expression). The temperature dependence of the rates, the solvent reorganization energies, and the deuterium kinetic isotope effects determined from the calculations are also consistent with the experimental results.

I. Introduction

Photosystem II (PSII) is a large membrane-bound protein complex that catalyzes the light-driven oxidation of water.[1−3] In this process, the absorption of light by the primary electron donor chlorophylls P680 leads to the transfer of an electron to a pheophytin and two quinones. Subsequently, a nearby tyrosyl residue Tyr_Z transfers an electron to the oxidized P680 and is thought to transfer its phenolic proton to a nearby base, leading to a neutral tyrosine radical. The Tyr_Z radical is then reduced by the abstraction of electrons from a tetranuclear Mn cluster bound to PSII. The oxidation of the Mn cluster has been postulated to involve hydrogen abstraction by the Tyr_Z radical rather than single electron transfer.[4−7] Four consecutive electron abstractions result in the oxidation of two water molecules and the production of one oxygen molecule. The detailed mechanism of charge separation in PSII is still not well understood.

In an effort to better understand the mechanism of PSII, Sjödin and co-workers have designed the model compound depicted in Figure 1 to mimic the PSII photochemistry.[8−11] In their experiments, photoexcitation of the ruthenium-tris-bipyridine leads to the transfer of an excited electron to the external acceptor methyl viologen. After this oxidative quenching, the tyrosine portion of the model compound transfers an electron to the ruthenium and is deprotonated. This deprotonation of the tyrosine occurs because the pK_a of tyrosine changes from 10 to −2 upon oxidation.[12] Sjödin and co-workers measured the pH dependence of the rate of electron transfer from tyrosine to ruthenium in this compound.[10,11] For pH below the tyrosine pK_a (pH < 10), the tyrosine is initially protonated, and the rate constant increases monotonically with pH. For pH < 10, the deuterium kinetic isotope effect was found to be $k_H/k_D = 2.0-2.5$.[11] For pH above the tyrosine pK_a (pH > 10), the tyrosine is initially deprotonated, and the rate increases 100-fold and becomes independent of pH. These results are consistent with the interpretation that the mechanism is proton-coupled electron transfer (i.e., concerted electron transfer and deprotonation) at pH < 10 but is single electron transfer for pH > 10. Furthermore, similar pH dependence and deuterium kinetic isotope effects have been observed for the analogous reaction

(1) A., D. B.; Babcock, G. T. In *Oxygenic Photosynthesis: The Light Reactions*; Yocum, C., Ed.; Kluwer: Dordrecht, The Netherlands, 1996; p 213.
(2) Debus, R. J. *Biochim. Biophys. Acta* **1992**, *1102*, 269.
(3) Barber, J.; Andersson, B. *Nature* **1994**, *370*, 31.
(4) Tommos, C.; Tang, X.-S.; Warncke, K.; Hoganson, C. W.; Styring, S.; McCracken, J.; Diner, B. A.; Babcock, G. T. *J. Am. Chem. Soc.* **1995**, *117*, 10325−10335.
(5) Hoganson, C. W.; Lydakis-Simantiris, N.; Tang, X.-S.; Tommos, C.; Warncke, K.; Babcock, G. T.; Diner, B. A.; McCracken, J.; Styring, S. *Photosynth. Res.* **1995**, *47*, 177.
(6) Hoganson, C. W.; Babcock, G. T. *Science* **1997**, *277*, 1953−1956.
(7) Blomberg, M. R. A.; Siegbahn, P. E. M.; Styring, S.; Babcock, G. T.; Akermark, B.; Korall, P. *J. Am. Chem. Soc.* **1997**, *119*, 8285−8292.
(8) Magnuson, A.; Berglund, H.; Korall, P.; Hammarström, L.; Akermark, B.; Styring, S.; Sun, L. *J. Am. Chem. Soc.* **1997**, *119*, 10720−10725.
(9) Magnuson, A.; Frapart, Y.; Abrahamsson, M.; Horner, O.; Akermark, B.; Sun, L.; Girerd, J.-J.; Hammarström, L.; Styring, S. *J. Am. Chem. Soc.* **1999**, *121*, 89−96.
(10) Sjödin, M.; Styring, S.; Akermark, B.; Sun, L.; Hammarström, L. *J. Am. Chem. Soc.* **2000**, *122*, 3932−3936.
(11) Sjödin, M.; Styring, S.; Akermark, B.; Sun, L.; Hammarström, L. *Philos. Trans. R. Soc. London B* **2002**, *357*, 1471−1479.
(12) Land, E. J.; Porter, G.; Fang, J. Y.; Strachan, E. *Trans. Faraday Soc.* **1961**, *57*, 1885−1893.

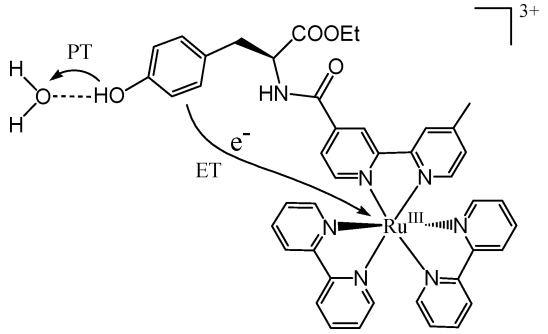

Figure 1. Schematic picture of the second step in the photochemical process for the model compound. In the first step, the ruthenium-tris-bipyridine portion absorbs light and the excited electron is transferred to an external methyl viologen acceptor. In the second step, the tyrosine portion transfers an electron to the ruthenium and is deprotonated.

in Mn-depleted PSII,[13] suggesting that the PSII mechanism also involves proton-coupled electron transfer from the tyrosine.

In this paper, we apply a multistate continuum theory for proton-coupled electron transfer (PCET)[14−16] to the model compound shown in Figure 1. The solute is represented by a multistate empirical valence bond model, the solvent is described by a dielectric continuum, and the transferring hydrogen nucleus is represented by a quantum mechanical wave function. We investigate the single ET reaction occurring at high pH:

$$(bpy)_2Ru^{III}-TyrO^{-}\cdots H_2O \rightleftarrows (bpy)_2Ru^{II}-TyrO\cdots H_2O \quad (1)$$

and the PCET reaction occurring at low pH:

$$(bpy)_2Ru^{III}-TyrOH\cdots H_2O \rightleftarrows (bpy)_2Ru^{II}-TyrO\cdots {}^{+}H_3O \quad (2)$$

where bpy denotes bipyridine and TyrOH denotes (4-Me-4′CONH-L-tyrosine ethyl ester-2,2′-bpy). We determine the structure with density functional theory and calculate the solvent reorganization energies with the frequency resolved cavity model. These theoretical calculations reproduce the experimentally determined relative rates of single ET and PCET, as well as the pH and temperature dependence of these reaction rates. An analysis of the results elucidates the detailed mechanism of the PCET reaction and provides an explanation for the substantially larger rate for single ET.

II. Theory and Methods

Fundamental Theory. PCET reactions have been studied with a variety of theoretical methods.[14−19] The theoretical formulation used to describe ET and PCET reactions in this paper is based primarily on the recently developed multistate continuum theory.[14−16] In this formulation, the solute is described by a multistate valence bond model, the transferring hydrogen nucleus is treated quantum mechanically, and the solvent is represented as a dielectric continuum. This theory may be used to calculate the free energy surfaces for single ET as a function of a single collective solvent coordinate or to calculate the free energy surfaces for PCET as functions of two collective solvent coordinates corresponding to PT and ET, respectively. The multistate continuum theory also provides rate expressions for ET and PCET reactions.

The single ET reaction in eq 1, which occurs at high pH, may be described in terms of the following two diabatic states:

$$(1)\ Ru^{III}-TyrO^{-}\cdots H_2O$$

$$(2)\ Ru^{II}-TyrO\cdots H_2O \quad (3)$$

The electron is transferred from the phenyl moiety of the tyrosine to the ruthenium. On the basis of the distance of electron transfer (≈10 Å) and the electronic properties of the system, this ET reaction is expected to be electronically nonadiabatic. The conventional unimolecular rate expression for nonadiabatic ET is[20−23]

$$k^{ET} = \frac{2\pi}{\hbar}|V_{12}|^2(4\pi\lambda k_B T)^{-1/2}\exp\left(\frac{-\Delta G^{\dagger}}{k_B T}\right) \quad (4)$$

where V_{12} is the coupling between the diabatic states, λ is the total reorganization energy, and $\Delta G^{\dagger}$ is the barrier defined as

$$\Delta G^{\dagger} = \frac{(\Delta G^{o} + \lambda)^2}{4\lambda} \quad (5)$$

The PCET reaction in eq 2, which occurs at low pH, may be described in terms of the following four diabatic states:

$$(1a)\ Ru^{III}-TyrOH\cdots H_2O$$

$$(1b)\ Ru^{III}-TyrO^{-}\cdots {}^{+}H_3O$$

$$(2a)\ Ru^{II}-TyrOH^{+}\cdots H_2O$$

$$(2b)\ Ru^{II}-TyrO\cdots {}^{+}H_3O \quad (6)$$

where 1 and 2 denote the ET state, and *a* and *b* denote the PT state. The proton is transferred from the oxygen atom of the tyrosine to the oxygen atom of the hydrogen-bonded water molecule, and the electron is transferred from the phenyl moiety of the tyrosine to the ruthenium. Within this notation, $1a \rightarrow 1b$ represents PT, $1a \rightarrow 2a$ represents ET, and $1a \rightarrow 2b$ represents EPT (where both the proton and the electron are transferred). Note that the ET reaction represented by these four PCET diabatic states involves complexes chemically different from those described for the single ET reaction due to the different protonation state of the tyrosine in the reactant.

As shown in ref 10, the free energy surfaces for PCET reactions may be calculated as functions of two collective solvent coordinates, z_p and z_e, corresponding to PT and ET, respectively. For the systems studied in this paper, the PT reaction is electronically adiabatic, while the ET/EPT reactions are electronically nonadiabatic. In this case, the ET diabatic free energy surfaces corresponding to ET states 1 and 2 are calculated as mixtures of the *a* and *b* PT states. The reactants (I) are mixtures of the 1*a* and 1*b* states, and the products (II) are mixtures of the 2*a* and 2*b* states. The proton vibrational states are calculated for both the reactant (I) and product (II) ET diabatic surfaces, resulting in two sets of two-dimensional vibrational-electronic free energy surfaces that may be approximated as paraboloids. In this theoretical formulation, the PCET reaction is described in terms of nonadiabatic transitions from the reactant (I) to the product (II) ET diabatic surfaces. (Here the

(13) Ahlbrink, R.; Haumann, M.; Cherepanov, D.; Bogershausen, O.; Mulkidjanian, A.; Junge, W. *Biochemistry* **1998**, *37*, 1131−1142.
(14) Soudackov, A.; Hammes-Schiffer, S. *J. Chem. Phys.* **1999**, *111*, 4672−4687.
(15) Soudackov, A.; Hammes-Schiffer, S. *J. Chem. Phys.* **2000**, *113*, 2385−2396.
(16) Hammes-Schiffer, S. *Acc. Chem. Res.* **2001**, *34*, 273−281.
(17) Cukier, R. I. *J. Phys. Chem.* **1996**, *100*, 15428.
(18) Cukier, R. I.; Nocera, D. G. *Annu. Rev. Phys. Chem.* **1998**, *49*, 337.
(19) Mayer, J. M.; Hrovat, D. A.; Thomas, J. L.; Borden, W. T. *J. Am. Chem. Soc.* **2002**, *124*, 11142−11147.
(20) Marcus, R. A.; Sutin, N. *Biochim. Biophys. Acta* **1985**, *811*, 265.
(21) Bixon, M.; Jortner, J. *Adv. Chem. Phys.* **1999**, *106*, 35.
(22) Barbara, P. F.; Meyer, T. J.; Ratner, M. A. *J. Phys. Chem.* **1996**, *100*, 13148.
(23) Newton, M. D.; Sutin, N. *Annu. Rev. Phys. Chem.* **1984**, *35*, 437.

ET diabatic states I and II, respectively, may be viewed as the reactant and product PCET states.)

The unimolecular rate expression derived in ref 11 for PCET is

$$k^{\mathrm{PCET}} = \frac{2\pi}{\hbar}\sum_{\mu} P_{\mathrm{I}\mu}\sum_{\nu}|V_{\mu\nu}|^2(4\pi\lambda_{\mu\nu}k_{\mathrm{B}}T)^{-1/2}\exp\left(\frac{-\Delta G^{\dagger}_{\mu\nu}}{k_{\mathrm{B}}T}\right) \quad (7)$$

where $\sum_{\mu}$ and $\sum_{\nu}$ indicate summations over vibrational states associated with ET states 1 and 2, respectively, $P_{\mathrm{I}\mu}$is the Boltzmann factor for state Iμ, and

$$\Delta G^{\dagger}_{\mu\nu} = \frac{(\Delta G^{\mathrm{o}}_{\mu\nu} + \lambda_{\mu\nu})^2}{4\lambda_{\mu\nu}} \quad (8)$$

In this expression the free energy difference is defined as

$$\Delta G^{\mathrm{o}}_{\mu\nu} = \epsilon^{\mathrm{II}}_{\nu}(\bar{z}^{\mathrm{II}\nu}_{\mathrm{p}},\bar{z}^{\mathrm{II}\nu}_{\mathrm{e}}) - \epsilon^{\mathrm{I}}_{\mu}(\bar{z}^{\mathrm{I}\mu}_{\mathrm{p}},\bar{z}^{\mathrm{I}\mu}_{\mathrm{e}}) \quad (9)$$

where $(\bar{z}^{\mathrm{I}\mu}_{\mathrm{p}},\bar{z}^{\mathrm{I}\mu}_{\mathrm{e}})$ and $(\bar{z}^{\mathrm{II}\nu}_{\mathrm{p}},\bar{z}^{\mathrm{II}\nu}_{\mathrm{e}})$ are the solvent coordinates for the minima of the ET diabatic free energy surfaces $\epsilon^{\mathrm{I}}_{\mu}(z_{\mathrm{p}},z_{\mathrm{e}})$ and $\epsilon^{\mathrm{II}}_{\nu}(z_{\mathrm{p}},z_{\mathrm{e}})$, respectively. Moreover, the outer-sphere (solvent) reorganization energy is

$$\lambda_{\mu\nu} = \epsilon^{\mathrm{I}}_{\mu}(\bar{z}^{\mathrm{II}\nu}_{\mathrm{p}},\bar{z}^{\mathrm{II}\nu}_{\mathrm{e}}) - \epsilon^{\mathrm{I}}_{\mu}(\bar{z}^{\mathrm{I}\mu}_{\mathrm{p}},\bar{z}^{\mathrm{I}\mu}_{\mathrm{e}}) = \epsilon^{\mathrm{II}}_{\nu}(\bar{z}^{\mathrm{I}\mu}_{\mathrm{p}},\bar{z}^{\mathrm{I}\mu}_{\mathrm{e}}) - \epsilon^{\mathrm{II}}_{\nu}(\bar{z}^{\mathrm{II}\nu}_{\mathrm{p}},\bar{z}^{\mathrm{II}\nu}_{\mathrm{e}}) \quad (10)$$

The coupling $V_{\mu\nu}$ in the PCET rate expression is defined as

$$V_{\mu\nu} = \langle\phi^{\mathrm{I}}_{\mu}|V(r_{\mathrm{p}},z^{\dagger}_{\mathrm{p}})|\phi^{\mathrm{II}}_{\nu}\rangle_{\mathrm{p}} \quad (11)$$

where the subscript of the angular brackets indicates integration over r_{p}, $z^{\dagger}_{\mathrm{p}}$ is the value of z_{p} in the intersection region, and ϕ^{I}_{μ} and ϕ^{II}_{ν} are the proton vibrational wave functions for the reactant and product ET diabatic states, respectively. For the system studied in this paper,

$$V_{\mu\nu} \approx V^{\mathrm{ET}}\langle\phi^{\mathrm{I}}_{\mu}|\phi^{\mathrm{II}}_{\nu}\rangle_{\mathrm{p}} \quad (12)$$

where V^{ET} is the electronic coupling between states 1*a* and 2*a* and between states 1*b* and 2*b*. The physical basis for this approximation is discussed in ref 20. This approximation is not used in the calculations of the rates, but it is useful in the analysis.

Although the effects of inner-sphere solute modes are easily included in this theoretical formulation,[15,24] experimental results imply that the inner-sphere reorganization energy does not contribute significantly to these types of reactions. Specifically, the Ru−N distances were found to be the same within experimental error for crystal structures of Ru(bpy)$_3^{3+}$ and Ru(bpy)$_3^{2+}$.[25] We also expect the inner-sphere reorganization within the tyrosine to be a relatively small effect. Thus, the reorganization energies used in the calculations for this paper include only outer-sphere (solvent) reorganization.

Calculating Input Quantities. Within the framework of the multistate continuum theory,[14] the calculation of the rates requires the gas phase valence bond matrix elements and the outer-sphere reorganization energies. The gas phase valence bond matrix elements are represented by molecular mechanical terms fit to available experimental data. The outer-sphere reorganization energy matrix elements are calculated with an electrostatic dielectric continuum model.

The calculation of both the gas phase and the solvation input quantities relies on obtaining qualitatively correct structures for the complex. For this purpose, we optimized the geometry of the Ru$^{\mathrm{II}}$(bpy)$_2$(4-Me-4′CONH-L-tyrosine ethyl ester-2,2′-bpy) complex (denoted Ru$^{\mathrm{II}}$TyrOH) with density functional theory (DFT) at the B3LYP/SBKJC(d) level.[26−29] This complex, which has a charge of +2 with a spin multiplicity of 1, represents the system prior to photoexcitation. Nuclear rearrangements upon photoexcitation and oxidative quenching are not expected to be significant for these calculations.[25] To determine the distance between the tyrosine oxygen and the closest water molecule oxygen, we optimized hydrogen-bonded complexes comprised of TyrOH or TyrO$^-$ and up to five water molecules at the B3LYP/6-31G** level[30−32] using the polarized continuum model (PCM).[33,34] The structure used in the multistate continuum theory calculations for the PCET reaction was based on the geometry obtained with three water molecules because the distance between the tyrosine and water oxygen atoms was converged to within the desired accuracy. The hydrogen-bonded water molecule was added to the structure of the optimized Ru$^{\mathrm{II}}$TyrOH complex by maintaining the optimized internal angles within the water molecule and between the water molecule and the tyrosine. The structure used in the multistate continuum theory calculations for the single ET reaction was based on the geometry obtained with only one water molecule, and in this case the results did not depend significantly on the location of the water. The optimization of Ru$^{\mathrm{II}}$-TyrOH was performed with GAMESS,[35] and all other DFT calculations were performed using Gaussian98.[36]

The gas phase valence bond matrix elements for the PCET reaction are based on a linear, five-site model:

$$\mathrm{O_A{-}H{-}O_D{-}Ph_D{-}Ru_A}$$

where the D and A subscripts denote donor and acceptor, respectively. The proton is transferred from the oxygen atom (O_D) of the tyrosine ligand to the oxygen atom (O_A) of the hydrogen-bonded water molecule. The electron is transferred from the phenyl moiety (Ph_D) of the tyrosine ligand to the ruthenium (Ru_A). The gas phase valence bond matrix elements are represented by molecular mechanical terms fit to electronic structure calculations and experimental data. The distances within this five-site model were determined from the DFT calculations described above, where the position of the Ph_D site was chosen to be the center of the phenyl ring of the tyrosine. The $O_A{-}O_D$, $O_D{-}Ph_D$, and $Ph_D{-}Ru_A$ distances are 2.63, 2.78, and 9.34 Å, respectively, for the PCET system. We emphasize that this five-site model is used only to provide molecular mechanical functional forms for the gas phase matrix elements. As described below, all atoms of the complex are included for the calculation of solvation properties.

The diagonal matrix elements are expressed as

(24) Iordanova, N.; Decornez, H.; Hammes-Schiffer, S. *J. Am. Chem. Soc.* **2001**, *123*, 3723−3733.
(25) Biner, M.; Burgi, H.-B.; Ludi, A.; Rohr, C. *J. Am. Chem. Soc.* **1992**, *114*, 5197−5203.
(26) Lee, C.; Yang, W.; Parr, P. G. *Phys. Rev. B* **1988**, *45*, 785.
(27) Becke, A. D. *J, Chem. Phys.* **1993**, *98*, 5648.
(28) Stephens, P. J.; Devlin, F. J.; Chablowski, C. F.; Frisch, M. J. *J. Phys. Chem.* **1994**, *98*, 11623.
(29) Stevens, W. J.; Krauss, M.; Basch, H.; Jasien, P. G. *Can, J. Chem.* **1992**, *70*, 612.
(30) Ditchfield, R.; Hehre, W. J.; Pople, J. A. *J. Chem. Phys.* **1971**, *54*, 724−728.
(31) Hehre, W. J.; Ditchfield, R.; Pople, J. A. *J. Chem. Phys.* **1972**, *56*, 2257−2261.
(32) Francl, M. M.; Pietro, W. J.; Hehre, W. J.; Binkley, J. S.; Gordon, M. S.; DeFrees, D. J.; Pople, J. A. *J. Chem. Phys.* **1982**, *77*, 3654−3665.
(33) Miertus, S.; Tomasi, J. *Chem. Phys.* **1982**, *65*, 239.
(34) Barone, V.; Cossi, M.; Tomasi, J. *J. Chem. Phys.* **1997**, *107*, 3210.
(35) Schmidt, M. W.; Baldridge, K. K.; Boatz, J. A.; Elbert, S. T.; Gordon, M. S.; Jensen, J. H.; Koseki, S.; Matsunaga, N.; Nguyen, K. A.; Su, S.; Windus, T. L.; Dupuis, M.; Montgomery, J. A. *J. Comput. Chem.* **1993**, *14*, 1347−1363.
(36) Frisch, M. J.; Trucks, G. W.; Schlegel, H. B.; Scuseria, G. E.; Robb, M. A.; Cheeseman, J. R.; Zakrzewski, V. G.; Montgomery, J., J. A.; Stratmann, R. E.; Burant, J. C.; Dapprich, S.; Millam, J. M.; Daniels, A. D.; Kudin, K. N.; Strain, M. C.; Farkas, O.; Tomasi, J.; Barone, V.; Cossi, M.; Cammi, R.; Mennucci, B.; Pomelli, C.; Adamo, C.; Clifford, S.; Ochterski, J.; Petersson, G. A.; Ayala, P. Y.; Cui, Q.; Morokuma, K.; Malick, D. K.; Rabuck, A. D.; Raghavachari, K.; Foresman, J. B.; Cioslowski, J.; Ortiz, J. V.; Babou, A. G.; Stefanov, B. B.; Liu, G.; Liashenko, A.; Piskorz, P.; Komaromi, I.; Gomperts, R.; Martin, R. L.; Fox, D. J.; Keith, T.; Al-Laham, M. A.; Peng, C. Y.; Nanayakkara, A.; Gonzalez, C.; Challacombe, M.; Gill, P. M. W.; Johnson, B.; Chen, W.; Wong, M. W.; Andres, J. L.; Gonzales, C.; Head-Gordon, M.; Replogle, E. S.; Pople, J. A. *Gaussian98*; Gaussian, Inc.: Pittsburgh, PA, 1998.

$$(h_o)_{1a,1a} = U^{\text{Morse}}_{O_DH} + U^{\text{rep}}_{O_AH} + U^{\text{Coul}}_{1a}$$

$$(h_o)_{1b,1b} = U^{\text{Morse}}_{O_AH} + U^{\text{rep}}_{O_DH} + U^{\text{Coul}}_{1b} + \Delta E_{1b}$$

$$(h_o)_{2a,2a} = U^{\text{Morse}}_{O_DH} + U^{\text{rep}}_{O_AH} + U^{\text{Coul}}_{2a} + \Delta E_{2a}$$

$$(h_o)_{2b,2b} = U^{\text{Morse}}_{O_AH} + U^{\text{rep}}_{O_DH} + U^{\text{Coul}}_{2b} + \Delta E_{2b} \qquad (13)$$

(Note that the dependence of the matrix elements on the proton coordinate is suppressed in eq 13 for clarity.) The Morse potential for an O−H bond of length R_{OH} is

$$U^{\text{Morse}}_{OH} = D_{OH}(1 - e^{-\beta_{OH}(R_{OH} - R^{o}_{OH})})^2 \qquad (14)$$

where $D_{OH} = 102$ kcal/mol, $\beta_{OH} = 2.35$ Å^{-1}, and $R^{o}_{OH} = 0.96$ Å. These values were chosen to be consistent with the experimental dissociation energy, frequency, and equilibrium bond length for typical O−H bonds.[37] The repulsion term between nonbonded atoms O and H separated by distance R_{OH} is

$$U^{\text{rep}}_{OH} = D'_{OH} e^{-\beta'_{OH} R_{OH}} \qquad (15)$$

where $\beta'_{OH} = 2.5$ Å^{-1} and $D'_{OH} = 500$ (1000) kcal/mol for tyrosine (water). These values were chosen to ensure correct asymptotic behavior of the gas phase diabatic energies along the hydrogen coordinate. The parameters for both the Morse and repulsion terms are similar to those used by Warshel and co-workers for related types of bonds.[37]

The Coulomb interaction potential between the transferring H atom and the other sites is

$$U^{\text{Coul}}_i = \sum_k \frac{q^i_k q_H e^2}{R_{kH}} \qquad (16)$$

where the summation is over all sites except the transferring hydrogen and the oxygen bonded to the hydrogen, R_{kH} is the distance between the hydrogen atom and site k, q_H is the charge assigned to the hydrogen, and q^i_k is the charge on site k for diabatic state i. For all diabatic states, the charge on the hydrogen is +0.5. The charge on Ph_D is 0 for ET state 1 and +1 for ET state 2, the charge on Ru_A is +3 for ET state 1 and +2 for ET state 2, the charge on O_D is −0.5 for PT state *a* and −1.0 for PT state *b*, and the charge on O_A is 0.0 for PT state *a* and +0.5 for PT state *b*.

The constants ΔE_{1b}, ΔE_{2a}, and ΔE_{2b} are fit to reproduce the experimentally determined driving forces (i.e., reaction free energies) for PT, ET, and PCET, respectively. The estimation of these quantities is based on the following experimental data:[10] the reduction potential for Ru(III) is +1.26 V (vs NHE),[38] the reduction potential for TyrOH is +0.93 V (vs NHE) at pH = 7,[39] the pK_a for TyrOH is 10,[12] and the pK_a for oxidized tyrosine ($TyrOH^+$) is −2.[10,12] As shown in Appendix A, the resulting reaction free energies are estimated to be

$$\Delta G^{\circ\prime\text{PT}}_{1a\rightarrow 1b} = 1.368(10 - \text{pH}) \text{ kcal/mol}$$

$$\Delta G^{\circ\text{ET}}_{1a\rightarrow 2a} = 4.65 \text{ kcal/mol}$$

$$\Delta G^{\circ\prime\text{EPT}}_{1a\rightarrow 2b} = -23.06(-0.083 + 0.059 \text{ pH}) \text{ kcal/mol} \qquad (17)$$

The reaction free energies for PT and PCET depend on pH to approximately account for the impact of bulk solvent on the proton transfer.[10] The parametrized constants ΔE_{1b}, ΔE_{2a}, and ΔE_{2b} are 202.94, −191.70, and 27.31 kcal/mol, respectively, at pH = 7.

In this paper, the couplings are assumed to be constant:

$$(h_o)_{1a,1b} = (h_o)_{2a,2b} = V^{\text{PT}}$$

$$(h_o)_{1a,2a} = (h_o)_{1b,2b} = V^{\text{ET}}$$

$$(h_o)_{1a,2b} = (h_o)_{1b,2a} = V^{\text{EPT}} \qquad (18)$$

The coupling $V^{\text{ET}} = 0.0027$ kcal/mol was determined by fitting to the experimental rate for the single ET reaction at high pH. For simplicity, in this paper the coupling for ET is assumed to be the same for the ET and PCET systems. The value of the coupling $V^{\text{PT}} = 33$ kcal/mol was chosen to be similar in magnitude to the couplings used in other related EVB models and was refined to fit the experimental rate for the PCET reaction at pH = 7. Within the model of valence bond theory, V^{EPT} is expected to be significantly smaller than V^{ET} since V^{EPT} is a second-order coupling and V^{ET} is a first-order coupling. For simplicity, in this paper V^{EPT} was approximated as zero. As given in eq 12, the overall coupling for a PCET reaction is approximately proportional to V^{ET} when $V^{\text{EPT}} = 0$.

The solvent reorganization energies are calculated with the frequency resolved cavity model (FRCM) developed by Newton, Rostov, and Basilevsky.[40,41] This approach allows for distinct effective solute cavities pertaining to the optical and inertial solvent response. The cavities are formed from spheres centered on all of the atoms. The two effective radii for the solute atoms are defined as $r_\infty = \kappa r_{\text{vdW}}$ and $r_{\text{in}} = r_\infty + \delta$, where r_{vdW} is the van der Waals radius, κ is a universal scaling factor, and δ is a constant specific to the particular solvent. As given in ref 36, $\kappa = 0.9$ and $\delta = 0.9$ for cations in water. The static and optical dielectric constants of water at 298 K are $\epsilon_o = 78.4$ and $\epsilon_\infty = 1.78$. As mentioned above, all atoms of the complex are included for the calculation of the solvation properties. The charge density of each diabatic (i.e., valence bond) state is defined by assigning appropriate partial charges to all atoms. The reorganization energy matrix element between diabatic states i and j is determined by calculating the interaction of the charge density of state i with the dielectric continuum solvent response to the charge density of state j.

The atomic coordinates utilized for the FRCM calculations were obtained from the DFT calculations described above. The atomic charges for the diabatic states used for the FRCM calculations in this paper were designated as follows. The ruthenium atom was assigned a charge of +2 or +3 corresponding to the appropriate oxidation state. The atomic charges on the bipyridyl ligands were obtained by optimizing the isolated ligands with density functional theory at the B3LYP/6-31G** level with C_{2v} symmetry and subsequently applying the CHELPG method[42] to the optimized ligands. The atomic charges for the tyrosine-containing ligand were chosen by optimizing the isolated ligand at the B3LYP/6-31G** level, assigning the appropriate charge and protonation state for each diabatic state, and calculating the atomic charges with the CHELPG method. The atomic charges for the 2*a* diabatic state were obtained as a function of the atomic charges in the other three diabatic states ($q_{2a} = q_{2b} - q_{1b} + q_{1a}$) to maintain consistent charge densities within the VB theory.[14] The atomic charges for the water molecules were obtained with the CHELPG method on the geometries optimized with the tyrosine. Note that this general assignment procedure neglects charge transfer between the ruthenium and the ligands. This simplification to the charge distribution does not qualitatively alter the calculated outer-sphere reorganization energies.

(37) Warshel, A. *Computer Modeling of Chemical Reactions in Enzymes and Solutions*; John Wiley & Sons: New York, 1991.
(38) Lin, C.-T.; Bottcher, W.; Chou, M.; Crreutz, C.; Sutin, N. *J. Am. Chem. Soc.* **1976**, *98*, 6536.
(39) Harriman, A. *J. Phys. Chem.* **1987**, *91*, 6102−6104.
(40) Basilevsky, M. V.; Rostov, I. V.; Newton, M. D. *Chem. Phys.* **1998**, *232*, 189−199.
(41) Newton, M. D.; Basilevsky, M. V.; Rostov, I. V. *Chem. Phys.* **1998**, *232*, 201−210.
(42) Breneman, C. M.; Wiberg, K. B. *J. Comput. Chem.* **1990**, *11*, 361.

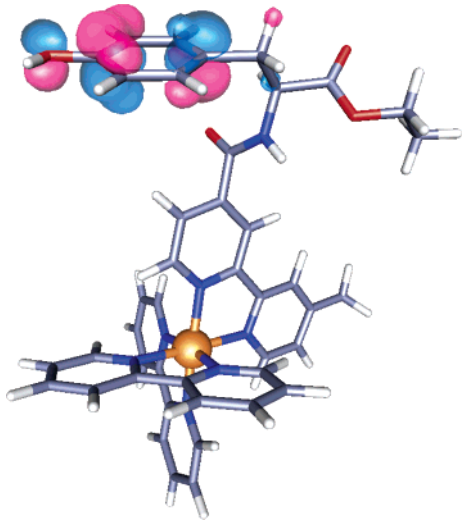

Figure 2. Structure of the $Ru^{II}(bpy)_2$(4-Me-4′CONH-L-tyrosine ethyl ester-2,2′-bpy) complex optimized at the B3LYP/SBKJC(d) level. The highest occupied molecular orbital, which is localized on the tyrosine, is also depicted.

Table 1. Calculated Solvent Reorganization Energies between the Indicated Diabatic States for the Single ET and PCET Reactions[a]

ET		PCET	
$\lambda^{ET}_{1\to2}$	$\lambda^{ET}_{1a\to2a}$	$\lambda^{PT}_{1a\to1b}$	$\lambda^{EPT}_{1a\to2b}$
21.7	21.6	6.9	31.6

[a] Energies are given in kcal/mol.

III. Results and Discussion

As described above, we performed DFT calculations to obtain the structure of the model compound for PSII. The geometry of the optimized Ru^{II}TyrOH complex at the B3LYP level is depicted in Figure 2. For the multistate continuum theory calculations, a water molecule was added to Figure 2 using the approach described above. Figure 2 also illustrates that the highest occupied molecular orbital for the Ru^{II}TyrOH complex is localized on the tyrosine phenyl moiety. This observation is consistent with the transfer of the electron from the tyrosine.

We investigated the single ET reaction that occurs at high pH. As shown in Table 1, we calculated the solvent reorganization energy to be $\lambda^{ET}_{1\to2} = 21.7$ kcal/mol with the FRCM method. This value agrees remarkably well with the reorganization energy of 22 kcal/mol determined experimentally by fitting the temperature dependence of the rate to the Marcus equation.[10,43] The reduction potential for TyrOH at pH > 10 (i.e., when it is initially deprotonated) is +0.72 V (vs NHE),[39] and the reduction potential of Ru(III) is +1.26 V (vs NHE).[38] As shown in Appendix A, the reaction free energy for the single ET reaction at pH > 10 is estimated to be $\Delta G° = -12.45$ kcal/mol. Note that this free energy of reaction is not the same as $\Delta G^{oET}_{1a\to2a}$ in eq 17, where the tyrosine is initially protonated, because the reduction potential is different for deprotonated and protonated tyrosine. Substituting the reorganization energy and reaction free energy into eq 4, we fit the electronic coupling to reproduce the experimentally measured rate for single ET (4.5×10^7 s^{-1}). The resulting electronic coupling is $V^{ET} = 0.0027$ kcal/mol. This coupling is much smaller than the thermal energy at room temperature and hence is consistent with the assumption that the reaction is electronically nonadiabatic.

We also investigated the PCET reaction that occurs at low pH. The solvent reorganization energies calculated with the FRCM method for the diabatic reactions are given in Table 1. Despite the difference in the protonation state of the tyrosine, the diabatic reorganization energy $\lambda^{ET}_{1a\to2a}$ for ET is consistent with the reorganization energy $\lambda^{ET}_{1\to2}$ calculated for the single ET reaction discussed above. The diabatic reorganization energy $\lambda^{EPT}_{1a\to2b}$ for EPT is larger than $\lambda^{ET}_{1a\to2a}$ for ET because the electron and proton are transferred in opposite directions in the PCET reaction, leading to greater charge separation in the solute for PCET. (As shown previously,[24,44] $\lambda^{EPT}_{1a\to2b} < \lambda^{ET}_{1a\to2a}$ when the electron and proton are transferred in the same direction.) Table 2 provides an analysis of the dominant contributions to the PCET rate expression in eq 7. The average deuterium kinetic isotope effect for pH < 10 was calculated to be $k_H/k_D \approx 3$, which is consistent with the experimental results of $k_H/k_D = 2.0-2.5$.

In addition, we compared the temperature dependence of the theoretical rates to the experimental data. Sjödin and co-workers determined the activation energies and the reorganization energies for single ET (high pH) and PCET (neutral pH) by fitting the experimental temperature dependence of the rate to the Marcus equation[10,43]

$$k = Ae^{-E_a/k_BT} \tag{19}$$

$$E_a = \frac{(\lambda + \Delta G^o)^2}{4\lambda} \tag{20}$$

As mentioned above, the reorganization energy determined experimentally for ET is in excellent agreement with the solvent reorganization energy for ET calculated with the FRCM method. Hence the temperature dependence of the theoretical ET rate calculated from eq 4 is consistent with the experimental data. The relation between the temperature dependence and the diabatic solvent reorganization energies is more complex for PCET due to mixing of the diabatic states and involvement of excited vibronic states. Figure 3 shows a plot of the temperature dependence for the theoretically calculated PCET rate at pH = 7 for 10−40 °C. (Since the dominant effect of temperature for this range is in the exponential of the rate expression in eq 7, the solute parameters and solvent dielectric constants are assumed to be independent of temperature.) A fit of this theoretical data to the single exponential in eq 19 leads to an effective activation energy of $E_a = 4.41$ kcal/mol. On the basis of eq 20 with $\Delta G^{o,EPT}_{1a\to2b} = -7.61$ kcal/mol from eq 17, this activation energy corresponds to an effective reorganization energy of 31 kcal/mol. This effective reorganization energy is consistent with the experimentally determined reorganization energy of 32 kcal/mol based on a similar analysis of the temperature-dependent data for neutral pH.[11,45] Thus, the

(43) Hammarström, L. Personal communication: The experimental reorganization energy for ET given in ref 10 was obtained using a reaction free energy of 0.77 eV rather than 0.72 eV. The reorganization energy increases from 0.9 to 0.95 eV when the correct reaction free energy of 0.72 eV is used.

(44) Iordanova, N.; Hammes-Schiffer, S. *J. Am. Chem. Soc.* **2002**, *124*, 4848−4856.

(45) The initial experimentally determined PCET reorganization energy at neutral pH was 46 kcal/mol,[10] but subsequently this experimentally determined value was modified to 32 kcal/mol by accounting for the mixing entropy of the released proton.[11]

Table 2. Analysis of the Dominant Contributions to the PCET Rate at 298 K for Three Different pH Values[a,b]

pH	R/P (μ/ν) state[c]	contribution to rate (%)	$\Delta G^0_{\mu\nu}$	$\lambda_{\mu\nu}$	$V^2_{\mu\nu}$	$\lvert\langle\varphi^{I}_{\mu}\rvert\varphi^{II}_{\nu}\rangle\rvert^2$	$e^{-\Delta G^{\ddagger}_{\mu\nu}/k_BT}$
5.5	1/1	63	−3.5	25.7	1.05×10^{-6}	0.179	3.10×10^{-4}
	1/2	32	1.2	22.4	5.37×10^{-6}	0.704	2.85×10^{-5}
	2/1	5	−8.9	22.3	5.74×10^{-6}	0.759	3.38×10^{-2}
7.0	1/1	72	−4.8	25.2	9.82×10^{-7}	0.149	9.21×10^{-4}
	1/2	19	0.7	22.5	5.60×10^{-6}	0.756	3.95×10^{-5}
	2/1	9	−9.2	22.5	5.48×10^{-6}	0.741	3.70×10^{-2}
9.0	1/1	84	−6.5	24.2	1.27×10^{-6}	0.207	4.28×10^{-3}
	1/2	5	0.0	22.8	5.11×10^{-6}	0.687	6.75×10^{-5}
	2/1	11	−9.7	23.2	4.19×10^{-6}	0.580	3.65×10^{-2}

[a] The reaction free energies, solvent reorganization energies, and couplings are for reactant and product PCET states that are mixtures of 1*a*/1*b* and 2*a*/2*b* diabatic states. [b] Energies are given in kcal/mol. [c] The R/P state refers to the indices of the reactant and product vibronic states.

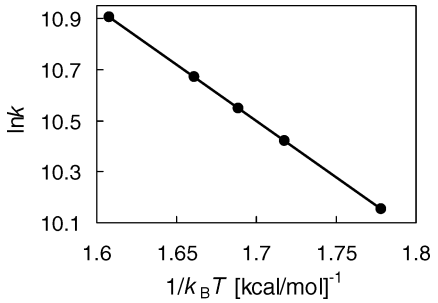

Figure 3. Theoretical data for the temperature dependence of the PCET rate k at pH = 7 for 10−40 °C. The slope of the straight line fit to the data is −4.405 kcal/mol, leading to a reorganization energy that is consistent with the value determined from the experimental temperature dependence of the rate.

temperature dependences of the theoretical and experimental rates are in excellent agreement for both ET and PCET.

The temperature dependence of the PCET rates is not directly related to the diabatic solvent reorganization energies due to mixing of the diabatic states. The reorganization energy $\lambda_{\mu\nu}$ used in the PCET rate expression (eq 7) is between the values for the diabatic ET and EPT reactions because the reactant and product PCET states are mixtures of the 1*a*/1*b* and 2*a*/2*b* diabatic states. Thus, the reorganization energies $\lambda_{\mu\nu} \approx 25$ kcal/mol for the dominant PCET channels given in Table 2 are smaller than the diabatic reorganization energy $\lambda^{\mathrm{EPT}}_{1a\rightarrow 2b} = 31.6$ kcal/mol given in Table 1. Table 2 indicates that the temperature dependence of the rate at neutral pH is dominated by a term in the rate expression (eq 7) corresponding to a reorganization energy of 25.2 kcal/mol and a reaction free energy of −4.8 kcal/mol. On the basis of eq 20, these values lead to an effective activation energy of $E_a = 4.1$ kcal/mol, which is similar to the slope of the theoretical data in Figure 3. The theoretical temperature dependence of the rate shown in Figure 3 is also consistent with the diabatic reorganization energy $\lambda^{\mathrm{EPT}}_{1a\rightarrow 2b} = 31.6$ kcal/mol and the diabatic reaction free energy $\Delta G^{o\prime\,\mathrm{EPT}}_{1a\rightarrow 2b} = -7.61$ kcal/mol, leading to an effective activation energy of $E_a = 4.6$ kcal/mol. In other words, similar effective activation energies are obtained from eq 20 with the diabatic EPT and mixed state values of the reorganization energy and reaction free energy. Thus, both the diabatic solvent reorganization energy calculated with the FRCM method and the effective reorganization energy determined from the temperature dependence of the theoretical rates agree with the reorganization energy of 32 kcal/mol determined from the temperature dependence of the experimental rates.[11,45] This observation is consistent with the dominance of the EPT mechanism, in which the electron and proton transfer simultaneously.

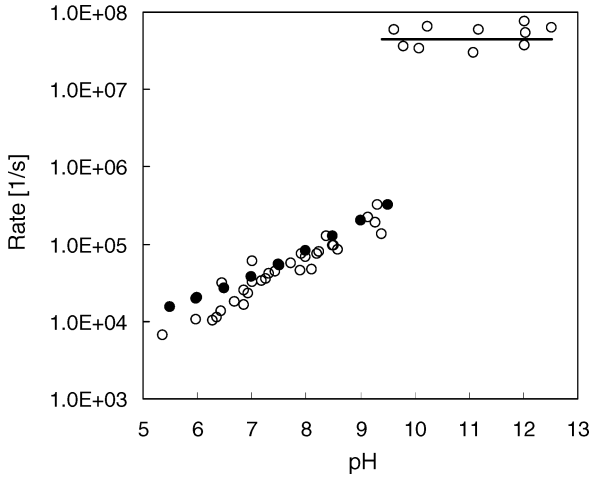

Figure 4. Experimental and theoretical data for the pH dependence of the rates for single ET and PCET. The experimental values are denoted with open circles. The theoretical PCET rates are denoted with filled circles, and the theoretical ET rate is represented by a solid line because it is independent of pH.

An additional complication arises in the analysis of the temperature dependence because the PCET rate given in eq 7 is a summation over reactant and product vibronic states. As shown in Table 2, although the transitions from the lowest reactant state to the lowest product state dominate the overall PCET rate, the transitions to and from the first excited states are also significant. The temperature dependence of each term is dominated by an exponential, but the relative weightings of the terms also depend on temperature. Therefore, fitting the experimental temperature dependence of the rate to a single exponential is not a rigorous method for calculating reorganization energies for PCET reactions. Nevertheless, Figure 3 indicates that this approximation is reasonable for this system.

The calculated and experimental pH dependences of the single ET and PCET rates are shown in Figure 4. Since the pH dependence of the rate is expected to be dominated by the pH dependence of the reaction free energies, the parameters ΔE_{1b} and ΔE_{2b} are varied with pH according to eq 17, while all other parameters are assumed to be independent of pH. Table 2 indicates that the calculated reorganization energies and couplings are similar for the range of pH = 5.5 to pH = 9.0, while the reaction free energies decrease significantly over this range. The rate of PCET increases monotonically with pH due to the decrease in these reaction free energies. The rate for single ET is independent of pH because the reaction free energy for single ET does not depend on pH.

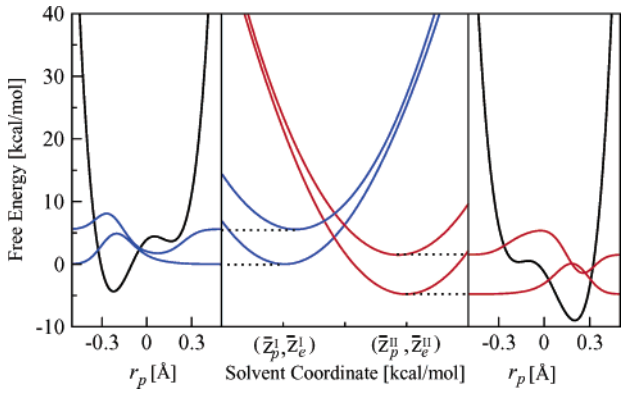

Figure 5. Analysis of the free energy surfaces for the PCET reaction in the model compound for PSII. In the center frame are slices of the two-dimensional ET diabatic free energy surfaces as functions of the solvent coordinates. The slices were obtained along the line connecting the minima of the lowest energy reactant (I) and product (II) two-dimensional free energy surfaces. In the left frame are the reactant (I) proton potential energy curve and the corresponding proton vibrational wave functions as functions of the proton coordinate r_p evaluated at the minimum of the ground state reactant free energy surface. In the right frame are the product (II) proton potential energy curve and the corresponding proton vibrational wave functions as functions of the proton coordinate r_p evaluated at the minimum of the ground state product free energy surface.

The calculations indicate that the substantially higher rate for single ET than for PCET is due to several factors. First, the solvent reorganization energy is smaller for single ET than for PCET. Second, the single ET reaction occurring at pH > 10 is more exoergic than the PCET reaction occurring at pH < 10. Third, the coupling for PCET is averaged over the reactant and product hydrogen vibrational wave functions (i.e., the vibrational overlap factor in eq 12), thereby decreasing the rate of PCET relative to single ET. This vibrational overlap factor arises from the motion of the transferring hydrogen. All three of these factors combine to enhance the rate for ET relative to PCET.

Figure 5 provides information about the detailed mechanism of PCET. This figure depicts the free energy profiles along the collective solvent coordinate and the proton potential energy curves with the corresponding proton vibrational wave functions. The minimum of the lowest reactant free energy profile is dominated by the 1*a* VB state, indicating that the ruthenium has oxidation state Ru(III) and the tyrosine is in its neutral form (TyrOH). The proton vibrational wave function is localized in the proton potential energy well near the tyrosine. In contrast, the minimum of the lowest product free energy profile is dominated by the 2*b* VB state, indicating that the ruthenium has oxidation state Ru(II) and the tyrosine is a radical (TyrO$^{\bullet}$). In this case, the proton vibrational state is localized in the proton potential energy well near the hydrogen-bonded water molecule. Table 2 indicates that the lowest energy reactant and product states are dominant for the relevant range of pH. These observations imply that the electron and proton transfer simultaneously in a coupled manner for this photoinduced reaction at pH < 10.

In contrast to previous dissociative descriptions involving a repulsive product state for the proton motion,[10,11,46] our description of the product state is limited to the initial proton transfer step from the tyrosine to the hydrogen-bonded water molecule. Immediately after the PCET reaction, the proton from the tyrosine is bound to the hydrogen-bonded water. Subsequently, a different proton on that water molecule is expected to be transferred to a neighboring water molecule, and the extra charge will diffuse throughout the bulk solution. In principle, these effects could be incorporated into our calculations with a multistate empirical valence bond potential including each protonation state of all water molecules in the bulk solvent.[47,48] To maintain a simple description, however, we incorporate the effect of the bulk solvent through the pH dependence of the reaction free energies. As shown above, this approximate description of the bulk solvent effects leads to excellent agreement between the theoretical and experimental data. A more rigorous treatment of these bulk solvent effects will be the topic of future investigations.

IV. Conclusions

We have applied a multistate continuum theory to a model for tyrosine oxidation in photosystem II. The calculations are consistent with the interpretation that the mechanism is PCET at pH < 10 when the tyrosine is initially protonated but is single ET for pH > 10 when the tyrosine is initially deprotonated. The single ET rate is independent of pH because the reaction free energy does not depend on pH, whereas the PCET rate increases monotonically with pH due to the decrease in the reaction free energies. The calculated pH dependence of the PCET rate for pH < 10 is in excellent agreement with the experimental data. The calculated deuterium kinetic isotope effect for pH < 10 is $k_H/k_D \approx 3$, which is consistent with the experimentally measured value of $k_H/k_D = 2.0-2.5$. Moreover, the experimentally measured relative rates of single ET and PCET are also reproduced by the theoretical calculations.

The calculated solvent reorganization energies and temperature dependences of the rates for ET and PCET are consistent with the experimental data. The diabatic solvent reorganization energy of 32 kcal/mol for PCET is larger than the diabatic solvent reorganization energy of 22 kcal/mol for single ET because the electron and proton are transferred in opposite directions in the PCET reaction, leading to greater charge separation in the solute for PCET. Analysis of the dominant contributions to the PCET rate expression indicates that the solvent reorganization energy is somewhat lower (≈25 kcal/mol) for the mixed vibronic PCET states, but concurrent changes in the reaction free energies lead to consistent temperature dependence of the rates. The transitions from the lowest reactant state to the lowest product state dominate the overall PCET rate, although the transitions to and from the first excited vibronic states are also significant. The overall analysis implies that the electron and proton transfer simultaneously in a coupled manner at pH < 10.

The calculations provide an explanation for the experimental observation that the rate of single ET is 2 orders of magnitude larger than the rate for PCET. This difference in rates arises from a combination of several factors. The smaller solvent reorganization energy and greater exoergicity for ET increase the rate for ET relative to PCET. In addition, the averaging of the coupling for PCET over the reactant and product hydrogen vibrational wave functions (i.e., the vibrational overlap factor in the PCET rate expression) decreases the rate of PCET relative

(46) Cukier, R. I. *J. Phys. Chem. A* **1999**, *103*, 5989−5995.
(47) Schmitt, U. W.; Voth, G. A. *J. Phys. Chem. B* **1998**, *102*, 5547−5551.
(48) Vuilleumier, R.; Borgis, D. *Chem. Phys. Lett.* **1998**, *284*, 71−77.

to ET. This overlap factor arises from the coupling between reactant and product vibronic states and plays a role similar to that of the Franck−Condon overlap factor in theories including quantum mechanical inner-sphere modes for single ET. The physical basis for this vibrational overlap factor is the motion of the transferring hydrogen.

This investigation provides further insight into the mechanism for tyrosine oxidation in a system designed to serve as a model for the analogous process in PSII. The pH dependence of the rate and the deuterium kinetic isotope effect for Mn-depleted PSII have been found experimentally to be similar to those properties of this model system.[13] Thus, the mechanistic understanding gained from these studies may also be applicable to PSII. Future calculations including the protein environment will lead to additional insights.

Acknowledgment. We gratefully acknowledge assistance from Leif Hammarström, who advised us concerning the calculation of the reaction free energies and supplied us with the experimental pH-dependent data. We also thank Alexander Soudackov for helpful discussions. This work was supported by NSF grant CHE-0096357 and NIH Grant GM56207.

Appendix

This appendix outlines the method for estimating the experimentally determined driving forces (i.e., reaction free energies) for ET, PT, and PCET. Note that the proton is transferred to bulk water. The impact of the bulk solvent is included in an approximate but physically meaningful manner through the pH dependence of the PT and PCET reaction free energies.[10]

Electron Transfer from Deprotonated Tyrosine to Ru(III). The electron transfer reaction from deprotonated tyrosine to Ru(III) is

$$\mathrm{TyrO^-} + \mathrm{Ru(III)} \rightarrow \mathrm{TyrO} + \mathrm{Ru(II)} \qquad \text{(A1)}$$

Equation A1 is the sum of eqs A2 and A3:

$$\mathrm{Ru(III)} + \mathrm{e^-} \rightarrow \mathrm{Ru(II)} \qquad \text{(A2)}$$

$$\mathrm{TyrO^-} \rightarrow \mathrm{TyrO} + \mathrm{e^-} \qquad \text{(A3)}$$

The reduction potential for eq A2 is $E° = 1.26$ V (vs NHE),[38] and the reduction potential for eq A3 is $E° = 0.72$ V (vs NHE).[39] Thus, the overall free energy of the reaction in eq A1 is

$$\Delta G^o = -23.061(1.26-0.72)\ \text{kcal/mol} = -12.45\ \text{kcal/mol}$$

Electron Transfer from Protonated Tyrosine to Ru(III). The electron transfer reaction from protonated tyrosine to Ru(III) is

$$\mathrm{TyrOH} + \mathrm{Ru(III)} \rightarrow \mathrm{TyrOH^+} + \mathrm{Ru(II)} \qquad \text{(A4)}$$

Equation A4 is the sum of eqs A5 and A6:

$$\mathrm{Ru(III)} + \mathrm{e^-} \rightarrow \mathrm{Ru(II)} \qquad \text{(A5)}$$

$$\mathrm{TyrOH} \rightarrow \mathrm{TyrOH^+} + \mathrm{e^-} \qquad \text{(A6)}$$

Equation A6 is the sum of eqs A7 and A8:

$$\mathrm{TyrOH} \rightarrow \mathrm{TyrO} + \mathrm{H^+} + \mathrm{e^-} \qquad \text{(A7)}$$

$$\mathrm{TyrO} + \mathrm{H^+} \rightarrow \mathrm{TyrOH^+} \qquad \text{(A8)}$$

The reduction potential for eq A5 is $E° = 1.26$ V (vs NHE).[38] The reduction potential of eq A7 is $E° = 0.93$ V (vs NHE)[39] at pH = 7, and therefore $E° = 0.93 + 0.059(7) = 1.343$ V (vs NHE) at pH = 0. The pK_a for $\mathrm{TyrOH^+}$ is −2,[10,12] so the free energy of the reaction in eq A8 is $\Delta G° = -1.368\ \mathrm{p}K_a$ kcal/mol = 2.736 kcal/mol at pH = 0. Therefore, the overall free energy of the reaction in eq A4 is $\Delta G^o = -23.061(1.26-1.343)$ kcal/mol + 2.736 kcal/mol = 4.65 kcal/mol.

Proton Transfer from Tyrosine to Water. The proton transfer reaction from protonated tyrosine to water is

$$\mathrm{TyrOH} + \mathrm{H_2O} \rightarrow \mathrm{TyrO^-} + \mathrm{H_3O^+} \qquad \text{(A9)}$$

The pK_a of TyrOH is 10,[12] so the free energy of this reaction is $\Delta G°' = 1.368\ (\mathrm{p}K_a - \mathrm{pH})$ kcal/mol = 1.368 (10 − pH) kcal/mol.

PCET from Tyrosine to Ru(III) and Water. The PCET reaction from tyrosine to Ru(III) is

$$\mathrm{TyrOH} + \mathrm{Ru(III)} + \mathrm{H_2O} \rightarrow \mathrm{TyrO} + \mathrm{Ru(II)} + \mathrm{H_3O^+} \qquad \text{(A10)}$$

Equation A10 is the sum of eqs A11 and A12:

$$\mathrm{Ru(III)} + \mathrm{e^-} \rightarrow \mathrm{Ru(II)} \qquad \text{(A11)}$$

$$\mathrm{TyrOH} + \mathrm{H_2O} \rightarrow \mathrm{TyrO} + \mathrm{H_3O^+} + \mathrm{e^-} \qquad \text{(A12)}$$

The reduction potential for eq A11 is $E° = 1.26$ V (vs NHE).[38] The reduction potential for eq A12 is $E° = 0.93$ V (vs NHE)[39] at pH = 7, and therefore $E° = 1.343 - 0.059$ (pH) V at general pH. Thus, the overall free energy for the reaction in eq A10 is $\Delta G°' = -23.061[1.26 - (1.343 - 0.059\ \mathrm{pH})]$ kcal/mol = $-23.061(-0.083 + 0.059\ \mathrm{pH})$ kcal/mol.

JA035588Z